Transient Analysis of Composite Plates with Different Types of Cutout

Dr.Muhsin J.Jweeg ***University of Al-Nahrain***

Dr.Riyah N.Kiter ***University of Anbar***

Mr.Ahmed N.Uwayed. ***University of Anbar***

Received on : 13/10/2010 ***Accepted on : 3/4/2012***

ABSTRACT

Composite laminate plates, fabricated by bonding fiber–reinforced layers, were dynamically analyzed under different combinations of number of layers, type of cutout, hole dimensions, angle of lamination and type of dynamic loading . This work was achieved by the well–known engineering software (ANSYS). The toughness of composite plates was evaluated in terms of the normal stress in the direction of loading at the periphery of the cutout. The toughness was found to increase by increasing the number of layers, by setting the lamination angle at around 40^{o},by selecting hole dimensions to width of plate ratio of around 0.4 and by employing square cutouts or avoiding triangular cutouts. Also, composite plates were found to be more strain-rate-sensitive in ramp loading, with least number of layers and with triangular type of cutout.

Keywords: dynamic, composite, plates, cutouts, finite elements, ANSYS.

1.INTRODUCTION:

With the increased application of composites in auto space structures, studies involving the assessment of the transient analysis of laminated composite plates receive attention of composite-structure designers and researchers.

Analytical solutions for the blast response of a foam-core composite sandwich panel were derived considering two phases of deformation: (a) core crushing during through-thickness wave propagation and (b) global panel bending/shear during transverse shear wave propagation. Global equilibrium equations of motion were formulated from the system Lagrangian and used to obtain transverse deflection and shear rotations. The predicted transient deformation of the sandwich panel was within 7% of FEA results using ABAQUS Explicit[1].

Numerous FEA programs were used to aid in the design process and to predict the performance and behavior of composite structures. Vibration testing as well as internal pressure testing to correlate the FEA models used in the design of a radome was performed by Shearography & Vibrometry and vacuum pressure test. The results were compared and used to validate the FEA model. The testing has corresponded accurately in comparison to the FEA model[2].

Equations were presented by A.L. Dobyns [3] for the analysis of simply supported orthotropic plates subjected to static and dynamic loading conditions. Transient loading conditions considered include sine, rectangular, and triangular pulses, and pulses representative of high explosive blast and nuclear blast. These pulses could apply as a uniform load over the panel, a concentrated load, a uniform load applied over a small rectangular area, and a cosine loading applied over a small rectangular area.

J.N Reddy [4] presented a finite-element analysis of the transient behavior of fiber-reinforced, single-layer and two- layer cross-ply rectangular plates of bi-modular materials (i.e. materials whose linear elastic properties depend on whether the fiber-direction strains are

tensile or compressive). To validate the finite element results a closed solution was presented for a rectangular plate with all edges simply supported and subjected to suddenly applied sinusoidally normal pressure. The time behavior of the transverse loading was arbitrary (e.g. Step, impulse, etc.).

J.N. Reddy [5] presented two different lamination schemes, under appropriate boundary conditions and sinusoidal distribution of the transverse load, the exact form of the spatial variation of the solution was obtained, and the problem was reduced to the solution of a system of ordinary differential equation in time, which were integrated numerically using Newmarkś direct integration method. Numerical results for deflections and stress were presented showing the effect of plate side-to thickness ratio, aspect ratio material orthotropy, and lamination scheme.

A shear- flexible finite element was employed by J.N. Reddy [6] to investigate the transient response of isotropic, orthotropic and layered anisotrpic composite plates. Numerical convergence and stability of the element was established by using Newmarks direct integration technique. Numerical results for deflection and stresses were presented for rectangular plates under various boundary conditions and loading. The parametric effects of the time step, finite element mesh, lamination scheme and orthotropy on the transient response were investigated.

The transient response of simply supported antisymmetric angle-ply rectangular plates subjected to arbitrary loading has been investigated by A.A. Khdeir & J.N.Reddy [7]. The state variable technique was used to solve exactly the equations of motion of the first-order transverse shear deformation theory (FSDT) as well as the classical lamination theory (CLPT). The solutions of these two theories were considered to bring out the influence of the transverse shear deformation, the degree of anisotropy, and the number of layers.

The dynamic response of orthotropic and transversely isotropic flat plates to dynamic transverse loading constitutes the main topic of Librescu,L. et al.[8]. The dynamic loading conditions considered include sine, rectangular and triangular pulses while spatially were considered as sinusoidally distributed. The results obtained as per a higher-order plate theory was compared with their first transverse shear deformation and classical counterparts. In addition, some results concerning the associated free-vibration and bi-axial buckling of such plates were presented and comparisons with some of the available results were undertaken.

Moayed R.M.[9] have developed the equations of motion of composite laminated plates (fabricated by bonding N fiber-reinforced layers together) to obtain deformations and stresses taking into account the dynamic load (function of time) with the presence of the effect of cutouts. Theoretical analysis by using the classical lamination theory (CLPT) was found to be inadequate for analysis of laminated composite plates because it neglects the effect of shear strain across the laminate thickness. He focused on the formulation of finite element relations as a computer oriented method for the transient response of composite multi layered plates, using a special third-order theory (HOST 7), which takes seven degrees-of freedom, by use of Newmarkś integration method. The numerical results show the parametric effects of aspect ratio, number of layers, lamination angle and orthotropy ratio.

The present work deals with the normal stress history as affected by the number of layers, lamination angle, hole dimensions to plate width ratio and the type of cutout

.

2.THEORETICAL CONSIDERATIONS:

In order that the present work would be self-contained, the following treatment was considered of direct relevance. The transformation equations for expressing stresses in an ***x-y*** coordinate system in terms of stresses in a 1-2 coordinate system, see **Fig.(1)**, are: [10]

$$\begin{Bmatrix}\sigma_x\\ \sigma_y\\ \tau_{xy}\end{Bmatrix}=\begin{bmatrix}\cos^2\theta & \sin^2\theta & -2\sin\theta\cos\theta\\ \sin^2\theta & \cos^2\theta & 2\sin\theta\cos\theta\\ \sin\theta\cos\theta & -\sin\theta\cos\theta & \cos^2\theta-\sin^2\theta\end{bmatrix}\begin{Bmatrix}\sigma_1\\ \sigma_2\\ \tau_{12}\end{Bmatrix} \quad (1)$$

Similarly, the strain transformation equations are:

$$\begin{Bmatrix}\varepsilon_x\\ \varepsilon_y\\ \frac{\gamma_{xy}}{2}\end{Bmatrix}=\begin{bmatrix}\cos^2\theta & \sin^2\theta & -2\sin\theta\cos\theta\\ \sin^2\theta & \cos^2\theta & 2\sin\theta\cos\theta\\ \sin\theta\cos\theta & -\sin\theta\cos\theta & \cos^2\theta-\sin^2\theta\end{bmatrix}\begin{Bmatrix}\varepsilon_1\\ \varepsilon_2\\ \frac{\gamma_{12}}{2}\end{Bmatrix} \quad (2)$$

Where it is observed that the strains do transform with the same transformation stresses if the tensor definition of shear strain is used (which is equivalent to the division of the engineering shear strain by two).

The implications of Kirchhoff-Love hypothesis on the laminate displacements u, v, and w in the x-, y-, and ***z-*** directions are derived by using the laminate cross section in the ***x-z*** plane shown in **Fig.(2).** The displacement, u, at any point z through the laminate thickness is

$$u=u_o-z\frac{\partial w_o}{\partial x} \quad (3)$$

By similar reasoning, the v, in the y-direction is

$$v=v_o-z\frac{\partial w_o}{\partial y} \quad (4)$$

The laminate strains have been reduced to $\varepsilon_x,\varepsilon_y$, and γ_{xy} by virtue of the Kirchhoff- Love hypothesis. That is, $\varepsilon_z=\gamma_{xz}=\gamma_{yz}=0$. For small strains (linear elasticity), the remaining strains are defined (after substituting the displacements u and v from Eq.(3) and (4)) as follows:

$$\varepsilon_x=\frac{\partial u}{\partial x}=\frac{\partial u_o}{\partial x}-z\frac{\partial^2 w_o}{\partial x^2}$$

$$\varepsilon_y=\frac{\partial v}{\partial y}=\frac{\partial v_o}{\partial y}-z\frac{\partial^2 w_o}{\partial y^2}$$

$$\gamma_{xy}=\frac{\partial u}{\partial y}+\frac{\partial v}{\partial x}=\frac{\partial u_o}{\partial y}+\frac{\partial v_o}{\partial x}-2z\frac{\partial^2 w_o}{\partial x\partial y} \quad (5)$$

Where the middle surface strains are :

$$\begin{Bmatrix}\varepsilon_x^o\\ \varepsilon_y^o\\ \gamma_{xy}^o\end{Bmatrix}=\begin{Bmatrix}\frac{\partial u_o}{\partial x}\\ \frac{\partial v_o}{\partial y}\\ \frac{\partial u_o}{\partial y}+\frac{\partial v_o}{\partial x}\end{Bmatrix} \quad (6)$$

and the middle surface curvature are

$$\begin{Bmatrix} k_x \\ k_y \\ k_{xy} \end{Bmatrix} = -\begin{Bmatrix} \dfrac{\partial^2 w_o}{\partial x^2} \\ \dfrac{\partial^2 w_o}{\partial y^2} \\ 2\dfrac{\partial^2 w_o}{\partial x \partial y} \end{Bmatrix} \tag{7}$$

The resultant laminate forces and moments acting on a laminate are obtained by integration of the stresses in each layer or lamina through the laminate thickness as:

$$N_x = \int_{-h/2}^{h/2} \sigma_x dz$$

$$M_x = \int_{-h/2}^{h/2} \sigma_x z dz \tag{8}$$

Actually, N_x is a force per unit length (width) of the cross section of the laminate as shown in **Fig.(3)** [10]. Similarly, M_x is a moment per unit length as shown in **Fig.(4)** [10]. The entire collection of force and moment resultants for an N-layered laminate is defined as:

$$\begin{Bmatrix} N_x \\ N_y \\ N_{xy} \end{Bmatrix} = \int_{-h/2}^{h/2} \begin{Bmatrix} \sigma_x \\ \sigma_y \\ \tau_{xy} \end{Bmatrix}_k dz = \sum_{k=1}^{N} \int_{z_{k-1}}^{z_k} \begin{Bmatrix} \sigma_x \\ \sigma_y \\ \tau_{xy} \end{Bmatrix}_k dz$$

$$\begin{Bmatrix} M_x \\ M_y \\ M_{xy} \end{Bmatrix} = \int_{-h/2}^{h/2} \begin{Bmatrix} \sigma_x \\ \sigma_y \\ \tau_{xy} \end{Bmatrix}_k z dz = \sum_{k=1}^{N} \int_{z_{k-1}}^{z_k} \begin{Bmatrix} \sigma_x \\ \sigma_y \\ \tau_{xy} \end{Bmatrix}_k z dz \tag{9}$$

Where z_k and z_{k-1} are defined in **Fig.(5)** [11]. Note that $z_0 = -h/2$; these forces and moment resultants do not depend on z after integration, but are functions of ***x*** and ***y***, the coordinates in the plane of the laminate middle surface.

The integration indicated in Eq.(9) can be rearranged to take advantage of the fact that the stiffness matrix for a lamina is constant within the lamina. Thus, the stiffness matrix goes outside the integration over each layer, but is within the summation of force and moment resultants for each layer. Thus Eq.(9) can be written as:

$$\begin{Bmatrix} N_x \\ N_y \\ N_{xy} \end{Bmatrix} = \begin{bmatrix} A_{11} & A_{12} & A_{16} \\ A_{12} & A_{22} & A_{26} \\ A_{16} & A_{26} & A_{66} \end{bmatrix} \begin{Bmatrix} \varepsilon_x^o \\ \varepsilon_y^o \\ \gamma_{xy}^o \end{Bmatrix} + \begin{bmatrix} B_{11} & B_{12} & B_{16} \\ B_{12} & B_{22} & B_{26} \\ B_{16} & B_{26} & B_{66} \end{bmatrix} \begin{Bmatrix} k_x \\ k_y \\ k_{xy} \end{Bmatrix}$$

$$\begin{Bmatrix} M_x \\ M_y \\ M_{xy} \end{Bmatrix} = \begin{bmatrix} B_{11} & B_{12} & B_{16} \\ B_{12} & B_{22} & B_{26} \\ B_{16} & B_{26} & B_{66} \end{bmatrix} \begin{Bmatrix} \varepsilon_x^o \\ \varepsilon_y^o \\ \gamma_{xy}^o \end{Bmatrix} + \begin{bmatrix} D_{11} & D_{12} & D_{16} \\ D_{12} & D_{22} & D_{26} \\ D_{16} & D_{26} & D_{66} \end{bmatrix} \begin{Bmatrix} k_x \\ k_y \\ k_{xy} \end{Bmatrix} \tag{10}$$

Where

$$A_{ij} = \sum_{k=1}^{N} \left(Q_{ij}\right)_k \left(z_k - z_{k-1}\right)$$

$$B_{ij} = \frac{1}{2} \sum_{k=1}^{N} \left(Q_{ij}\right)_k \left(z_k^2 - z_{k-1}^2\right)$$

$$D_{ij} = \frac{1}{3} \sum_{k=1}^{N} \left(Q_{ij}\right)_k \left(z_k^3 - z_{k-1}^3\right) \tag{11}$$

For laminates that are symmetric in both geometry and material properties about the middle surface, the general stiffness equations, Eq.(11), are simplified considerably. In particular, because of the symmetry of the $\left(Q_{ij}\right)_k$ and the thickness h_k all the coupling stiffness, that is, the B_{ij}, can be shown to be zero. The force and moment resultants for a symmetric laminate are:

$$\begin{Bmatrix} N_x \\ N_y \\ N_{xy} \end{Bmatrix} = \begin{bmatrix} A_{11} & A_{12} & A_{16} \\ A_{12} & A_{22} & A_{26} \\ A_{16} & A_{26} & A_{66} \end{bmatrix} \begin{Bmatrix} \varepsilon_x^0 \\ \varepsilon_x^0 \\ \gamma_{xy}^0 \end{Bmatrix}$$

$$\begin{Bmatrix} M_x \\ M_y \\ M_{xy} \end{Bmatrix} = \begin{bmatrix} D_{11} & D_{12} & D_{16} \\ D_{12} & D_{22} & D_{26} \\ D_{16} & D_{26} & D_{66} \end{bmatrix} \begin{Bmatrix} k_x \\ k_x \\ k_{xy} \end{Bmatrix} \tag{12}$$

The equilibrium differential equations in terms of the moment and force resultants for a plate element are [5]:

$$\begin{aligned} N_{x,x} + N_{xy,y} &= I_1 u_{,n} + I_2 \phi_{x,u} \\ N_{xy,x} + N_{y,y} &= I_1 v_{,u} + I_2 \phi_{y,u} \\ Q_{x,x} + Q_{y,y} &= I_1 w_{,u} + q\left(x, y, t\right) \\ M_{x,x} + M_{xy,y} - Q_x &= I_3 \phi_{x,u} + I_2 u_{,u} \\ M_{xy,x} + M_{y,y} - Q_y &= I_3 \phi_{y,u} + I_2 v_{,u} \end{aligned} \tag{13}$$

Where a comma denotes differentiation of principal symbol with respect to the subscript, $q\left(x, y, t\right)$ is the applied load and I_1, I_2, I_3, are the normal, coupled normal-rotary and rotary inertia coefficients, defined as:

$$\left(I_1, I_2, I_3\right) = \int_{-h/2}^{h/2} \rho\left(1, z, z^2\right) dz = \sum_{k=1}^{N} \int_{z_{k-1}}^{z_k} \rho^{(k)} \left(1, z, z^2\right) dz \tag{14}$$

3.MODELING PROCEDURE:

The normal stress history at point (A), **Fig.(6)** , was determined for symmetric square plates consisting of various numbers of layers, (D/2b) ratio and different types of cutout, ,

subjected to step, ramp and exponential loading as shown in **Fig.(7).** The material properties were selected close to the low-modulus graphite-epoxy composite material; these are :

E_1= 132 (GPa), E_2= 10.7 (GPa)

G_{12}= G_{13}= G_{23}= 3.6 (GPa), ν12 = 0.24, ρ = 3.54 (Kg /m^3).

4.RESULTS AND DISCUSSION:

Figs.(8, 9 & 10) show the response of symmetric square plates, containing central circular hole, to step, ramp and exponential loading for different number of layers of angle–ply ($0^\circ/0^\circ$/-----/0°). The response is presently evaluated in terms of the normal stress (σ_x) at point (A) of a symmetric square plate shown in **Fig.(6).** In these figures, the plate consisting of the higher number of layers exhibits the lower value of normal stress. The number of layers effect on the extensional, coupling and binding toughness can be predicted from Eq.(11). Moreover, the transient response to the step loading is apparent , see **Fig.(8).**

Figs.(11, 12 & 13) show the response of symmetric square plates containing central circular hole , made with different angles of lamination subjected to step loading for different number of layers. Also, **Figs.(14, 15 & 16)** show the response of symmetric square plates containing central circular hole , made with different angles of lamination but in this case subjected to ramp loading for different number of layers. Finally, **Figs.(17, 18 & 19)** show the response of symmetric square plates containing central circular hole , made with different angles of lamination subjected to exponential loading for different number of layers. In all these figures **Figs.(11)** through **(19)** , the increase of lamination angle seems to increase the normal stress to a maximum at $\theta = 20^\circ$ beyond which the stress decreases drastically at $\theta = 40^\circ$.

Figs.(20) through **(28)** show the effect of (D/2b) ratio of angle–ply ($0^\circ/0^\circ$/-----/0°) on the variation of normal stress of symmetric square plates, consisting of (4, 6 and 8) layers and containing central circular hole, subjected to step, ramp and exponential loading. In these figures, the normal stress is shown to have a critical value at (D/2b=0.2).

Figs.(29, 30 & 31) show the effect of type of cutout (circular, square, hexagonal and triangular) of angle–ply ($0^\circ/0^\circ/0^\circ/0^\circ$) on the variation of normal stress of symmetric square plates, consisting of (4) layers and containing central circular hole, subjected to step, ramp and exponential loading. In these figures, the value of normal stress for triangular hole is the highest among that for others (square, hexagonal and even circular holes). The lower value of stress is attained with square holes.

Finally, **Tables(1, 2 & 3**) give the dynamic load factor (D.L.F) of symmetric square plates, consisting of (2, 4 & 6) layers of angle–ply ($0^\circ/0^\circ/0^\circ/0^\circ$) and containing various types of cutouts, subjected to step, ramp and exponential dynamic loading. In these tables, the value of (D.L.F) has a critical value when the loading is ramp, or when the hole is triangular and when the number of layers is 2 layers of angle-ply ($0^\circ/0^\circ/0^\circ/0^\circ$) of the same thickness.

5.CONCLUSIONS:

From the previous discussion, the following can be concluded:

1- The extensional, coupling and binding toughness increase as the number of layers increases in a symmetric square plate subjected to uniaxial dynamic loading.

2- The normal stress is increased to a maximum at $\theta = 20^\circ$ beyond which the stress decreases drastically at $\theta = 40^\circ$.
3- The increase of hole dimensions to width of plate ratio above (D/2b=0.1) raises the value of normal stress abruptly when the hole size is doubled beyond which the stress is reduced at (D/2b=0.4) even lower than the original value at (D/2b=0.2).
4- The toughness of square plates increases as the cutout changes from square to circular to hexagonal to triangular.
5- The dynamic load factor, and hence the strain rate sensivity, increases as the loading changes from step to exponential to ramp, or as the hole size changes from square to circular to triangular and finally as the number of layers changes from 6 to 4 to 2 layers.

6.REFRENCES:

[1]. L.P. Palla,(Blast Response of Composite Sandwich Panels), M.Sc. thesis. University of Akron, (2008).
[2]. J. Bail,(Non-destructive Investigation & FEA Correlation on an Aircraft Sandwich Composite Structure)), M.Sc. thesis. University of Akron, (2007).
[3]. A.L. Dobyns, (Analysis of Simply – Supported Orthotropic Plates Subjected To Static and Dynamic Loads), AIAA J., Vol. 19, No. 3, P.P. 642 – 650, may (1981).
[4]. J.N. Reddy, (Transient Response of Laminated Bi-modular – Material, Composite Rectangular Plates), J. Composite Materials, 16 (1982), P.P. 139.
[5]. J.N. Reddy, (On The Solutions To Forced Motions of Rectangular Composite Plates), J. Applied Mechanics, ASME, Vol. 49, P.P. 403 - 408, June (1982).
[6]. J.N. Reddy, (Dynamic [Transient] Analysis of Laminated an Isotropic Composite – Material Plates), Int. J. Numerical Methods In Engineering, Vol. 19, P.P. 237 – 255, (1983).
[7]. A.A. Khdeir & J.N. Reddy, (Dynamic Response of Antisymmetric Angle – Ply Laminated Plates Subjected To Arbitrary Loading) J. Sound & Vibration, 126 (3), P.P. 437 – 445, (1988).
[8]. L.Librescu, A.A. Khdeir & J.N. Reddy, (Further Results Concerning The Dynamic Response of Shear Deformable Elastic Orthotropic Plates), ZAMMZ. Angew Math. Mech.70(1990), P.P. 23 – 33.
[9]. M.R. Mahl, (Investigation of The Transient Response of Composite Laminated Plates Including The Effect of Cutout), M.Sc.Thesis, Baghdad University, College of Eng., department of Mechanical Eng., (2000).
[10].L.R. Calcote (The Analysis of Lamination Composite Structures) Van Nostran Reinholed Company [1969].
[11]. Robert M. Jones, (Mechanics of Composite Materials), McGraw- Hill Book Company, (1975).

7.NOMENCLATURE:

Extension stiffness elements	A_{ij}
Bending-extension coupling stiffness elements	B_{ij}
Bending stiffness elements	D_{ij}
Inertia of laminated plate	I
Layer number	k
Normal and twisting moments per unit length	M
Stress resultants	N_i
Number of laminate layers	N

Normal pressure	q
Transformed stress-strain relation from principal to laminate coordinates	Q_{ij}
Shear forces	Q_x,Q_y
Stress resultants	N_i
Time	t
Displacements	u,v,w
Middle surface displacements	u_o,v_o,w_o
Rectangular coordinates	x,y,z
Slope of laminate middle surface	β
Shearing strain	γ_{ij}
Middle surface shear strain	γ_o
Normal strain	ε
Middle surface strain	ε_o
Angle of lamination	θ
Material mass density	ρ
Normal stress	σ
Shearing stress	τ
Cross sectional rotation of the transverse normal	Φ

Table (1): Dynamic Load Factor (DLF) for (step , ramp & exponential) load of symmetric square plates (2- layers) with different types of cutouts.

D.L.F = $\sigma_x \mid dynamic / \sigma_x \mid static$			*Type of cutout*
Exponential load	*Ramp load*	*Step load*	
3.188	3.35	2.35	-
3.45	3.645	2.565	Circular
3.51	3.68	2.457	Square
3.365	3.39	2.499	Hexagonal
3.11	3.271	3.677	Triangular

Table (2): Dynamic Load Factor (DLF) for (Step , ramp & exponential) load of symmetric square plates (4- layers) with different types of cutouts.

D.L.F = $\sigma_x \mid dynamic / \sigma_x \mid static$			*Type of cutout*
Exponential load	*Ramp load*	*Step load*	
2.135	2.45	1.15	-
2.352	2.567	1.453	Circular
2.423	2.573	1.454	Square
2.281	2.497	1.485	Hexagonal
2.951	3.271	2.677	Triangular

Table (3): Dynamic Load Factor (DLF) for (step, ramp & exponential) load of symmetric square plates (6- layers) with different types of cutouts.

D.L.F = $\sigma_x \mid dynamic / \sigma_x \mid static$			*Type of cutout*
Exponential load	*Ramp load*	*Step load*	
1.215	1.85	1.02	-
1.399	1.772	1.235	Circular
1.382	1.785	1.228	Square
1.145	1.524	1.126	Hexagonal
1.841	2.186	1.989	Triangular

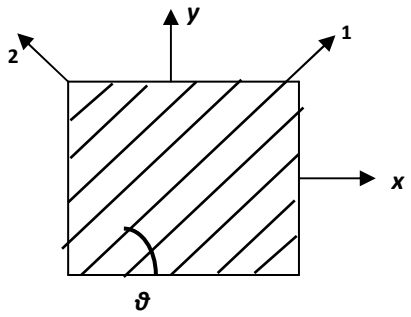

Figure (1): Lamina of arbitrary orientation of principal material directions.

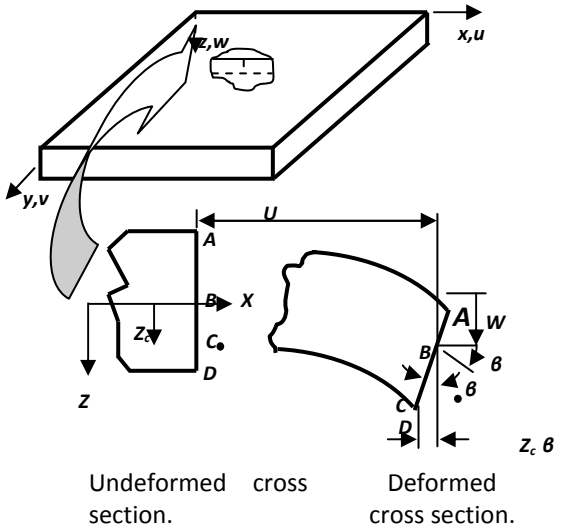

Figure(2): Geometry of deformation.

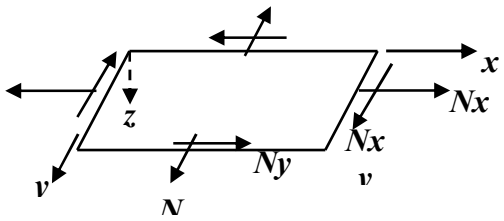

Figure(3): In-plane on a flat laminate .

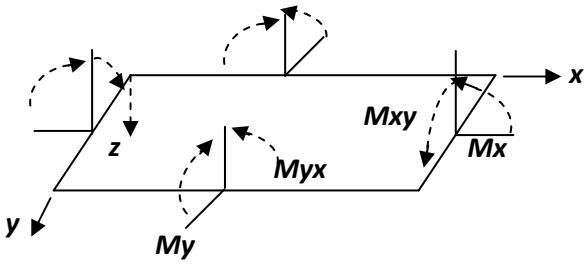

Figure (4): Moments on a flat laminate **.**

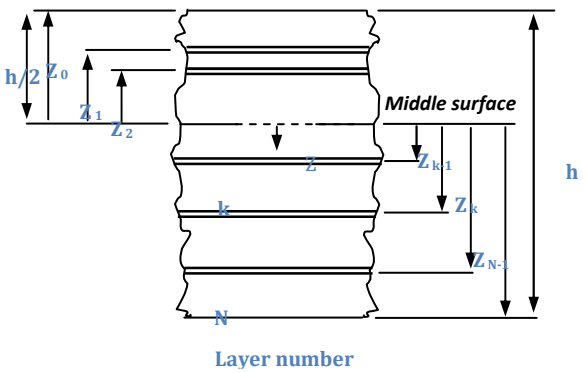

Figure(5): Geometry of an n-layered laminate**.**

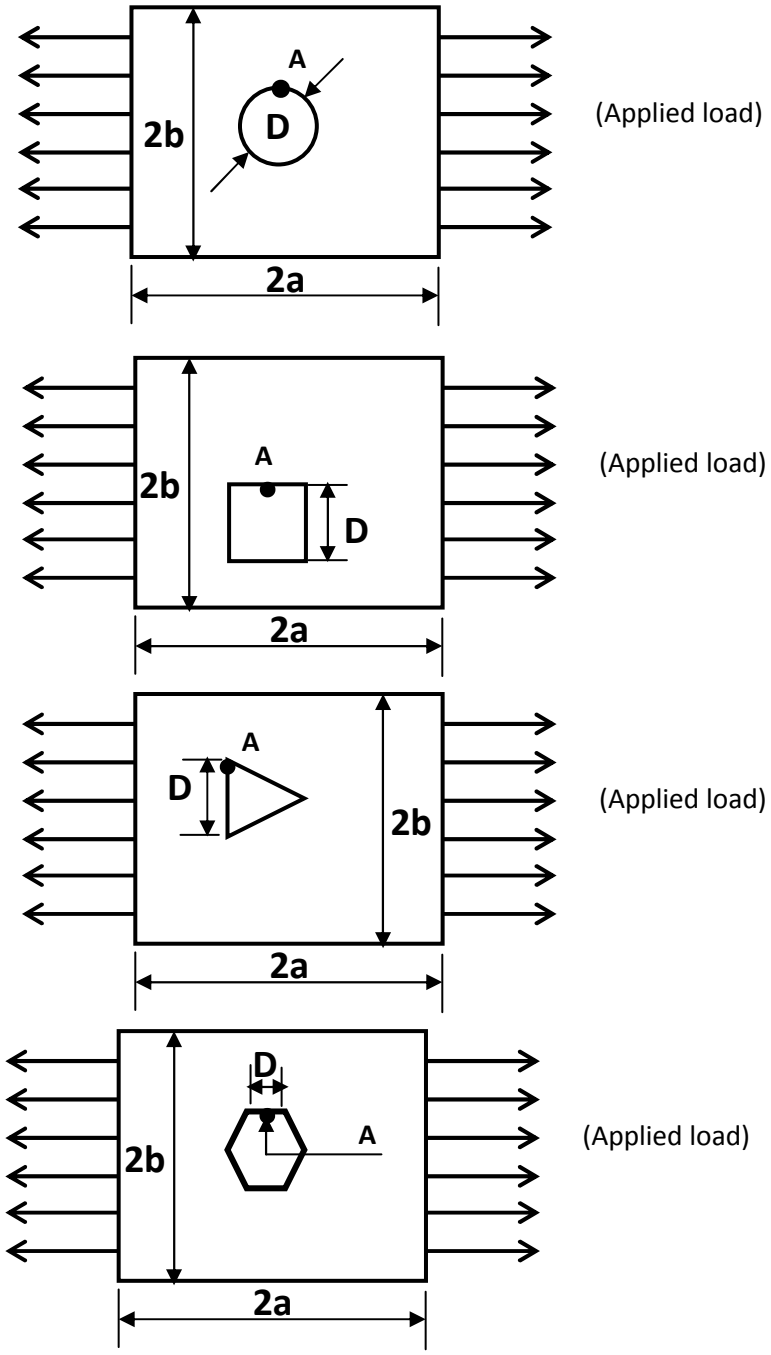

Figure(6): Square plates with central holes subjected to dynamic loading.

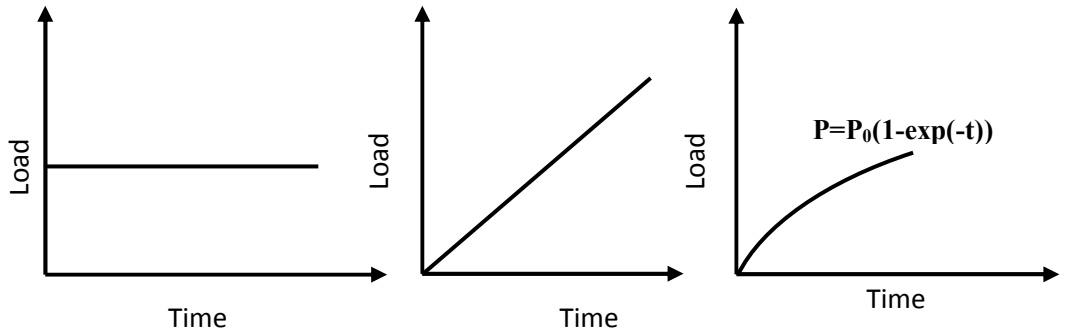

Figure(7): Types of dynamic loadings.

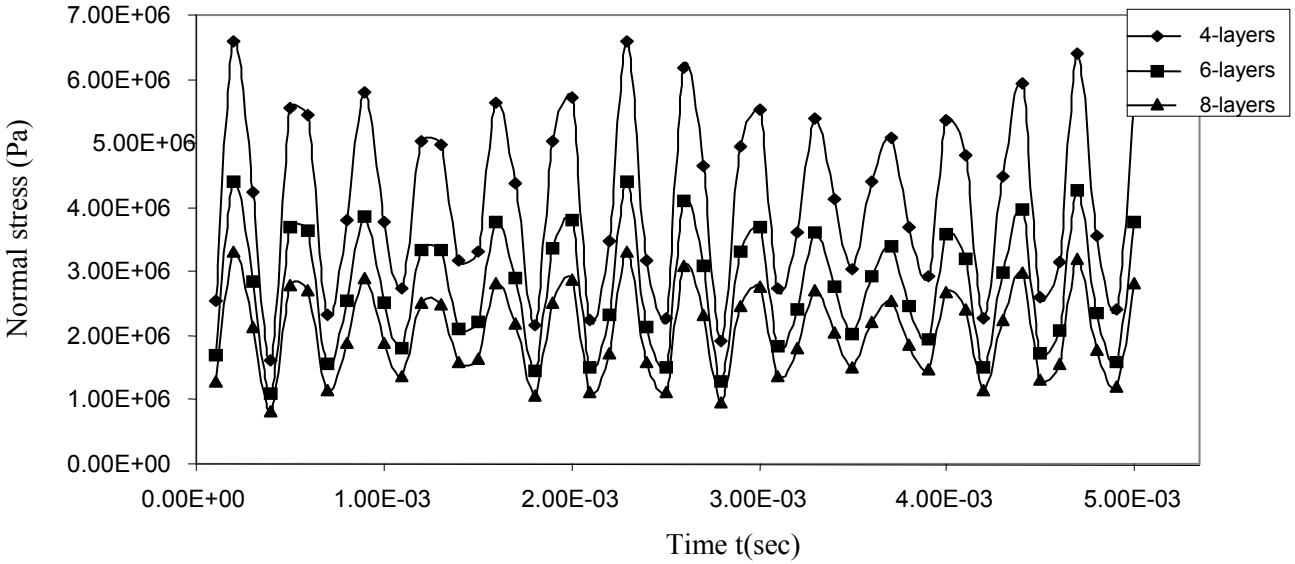

Figure(8):The effect of number of layers on the variation of the normal stress at point (A) of a symmetric square plate with central circular hole under step-load.

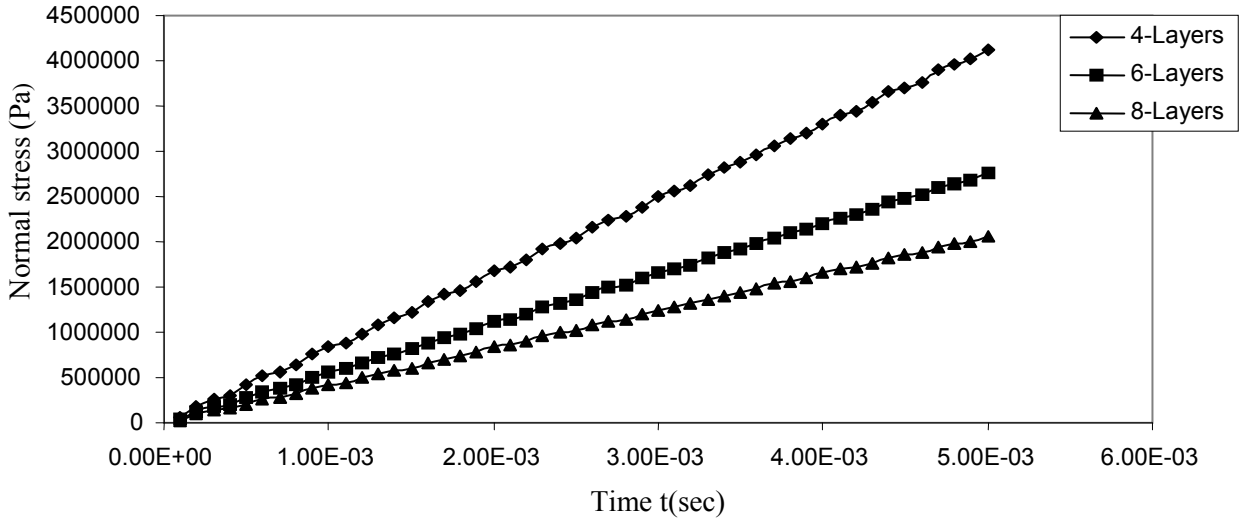

Figure(9):The effect of number of layers on the variation of the normal stress at point (A) of a symmetric square plate with central circular hole under ramp-load.

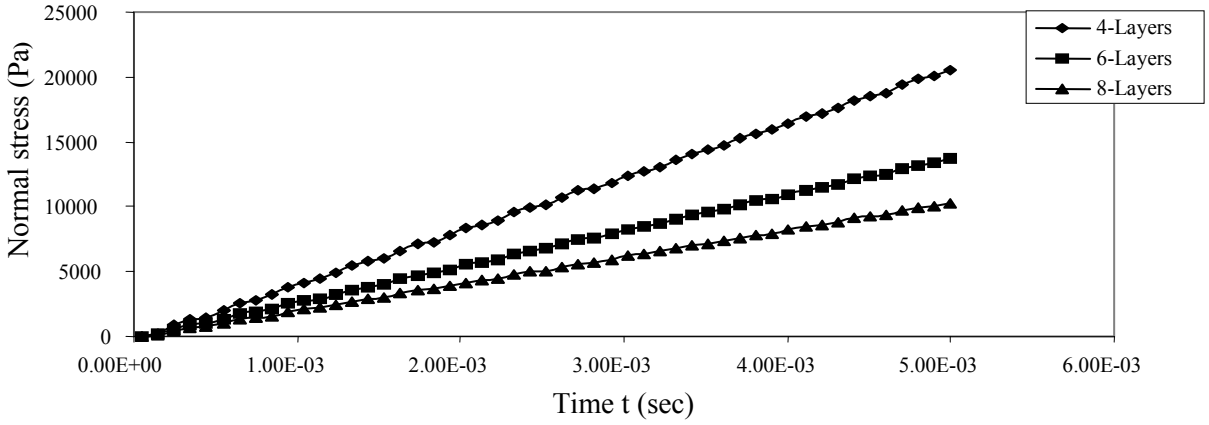

Figure(10): The effect of number of layers on the variation of the normal stress at point (A) of a symmetric square plate with central circular hole under exponential load.

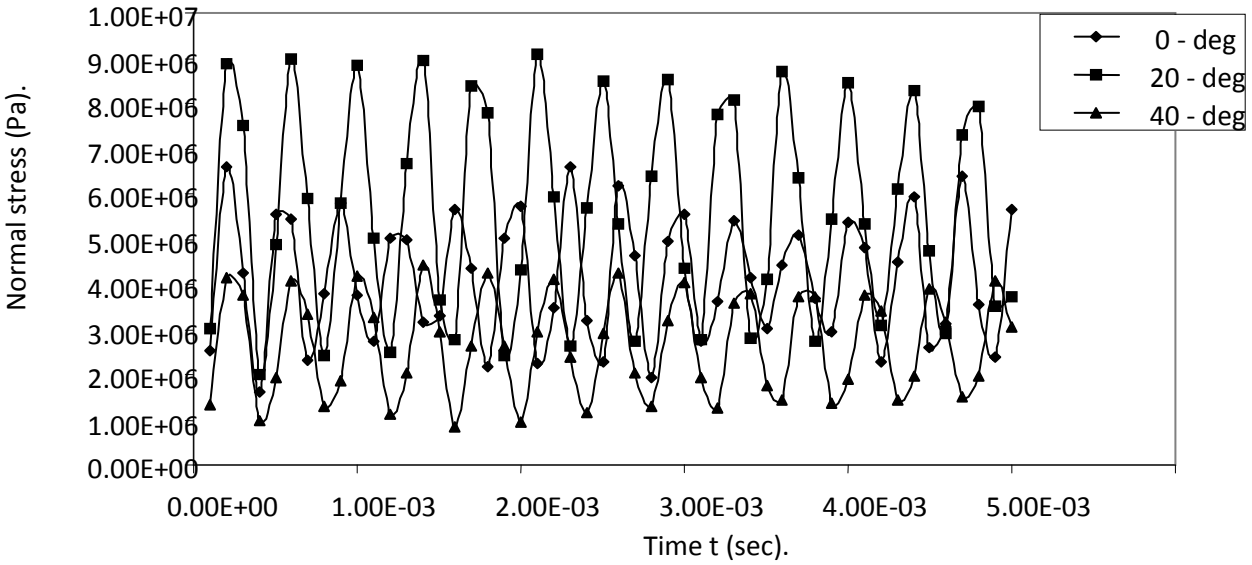

Figure(11):The effect of the lamination angle on the variation of normal stress at point (A) of square symmetric plate(4– Layers) with central circular hole under step-load.

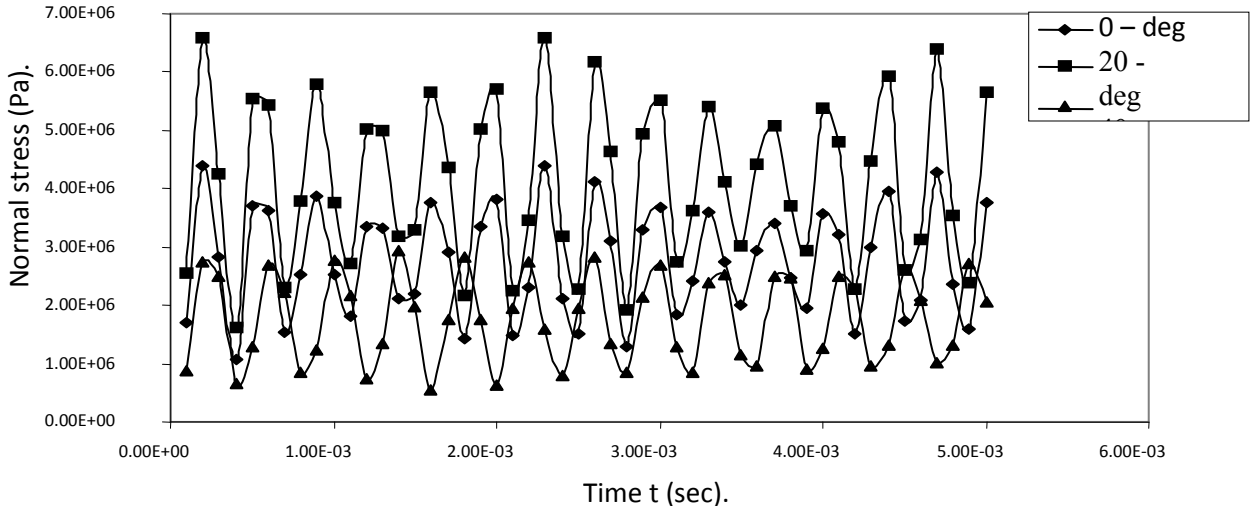

Figure(12):The effect of the lamination angle on the variation of normal stress at point (A) of square symmetric plate(6– Layers) with central circular hole under step-load.

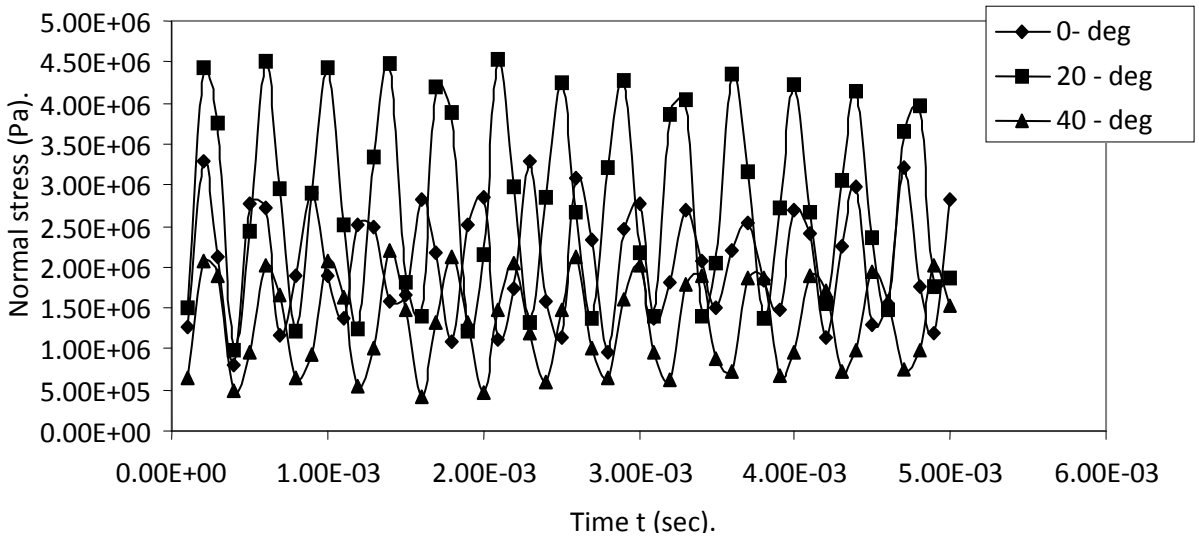

Figure(13): The effect of the lamination angle on the variation of normal stress at point (A) of square symmetric plate(8– Layers) with central circular hole under step-load.

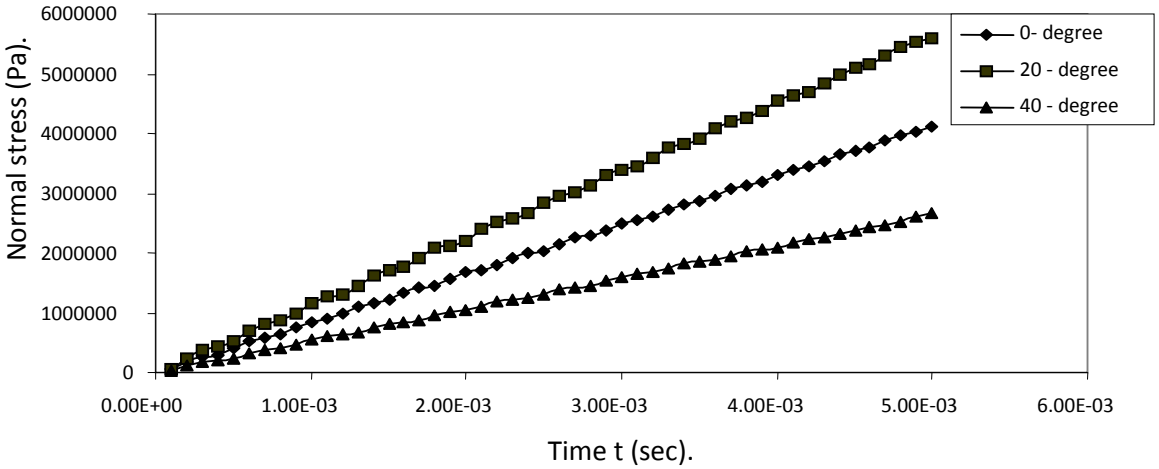

Figure(14): The effect of the lamination angle on the variation of normal stress at point (A) of square symmetric plate(4– Layers) with central circular hole under ramp-load.

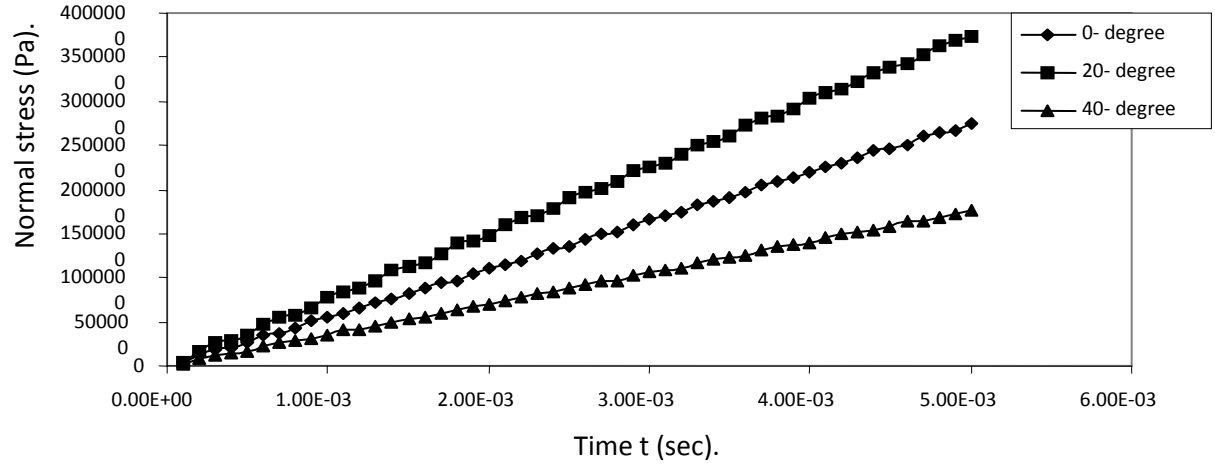

Figure(15): The effect of the lamination angle on the variation of normal stress at point (A) of square symmetric plate(6– Layers) with central circular hole under ramp-load.

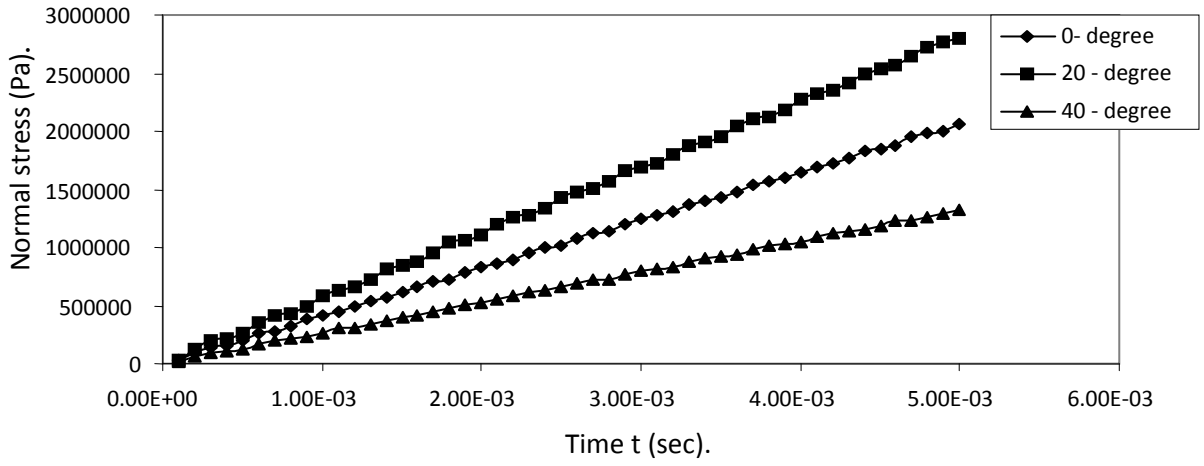

Figure(16):The effect of the lamination angle on the variation of normal stress at point (A) of square symmetric plate(8– Layers) with central circular hole under ramp-load.

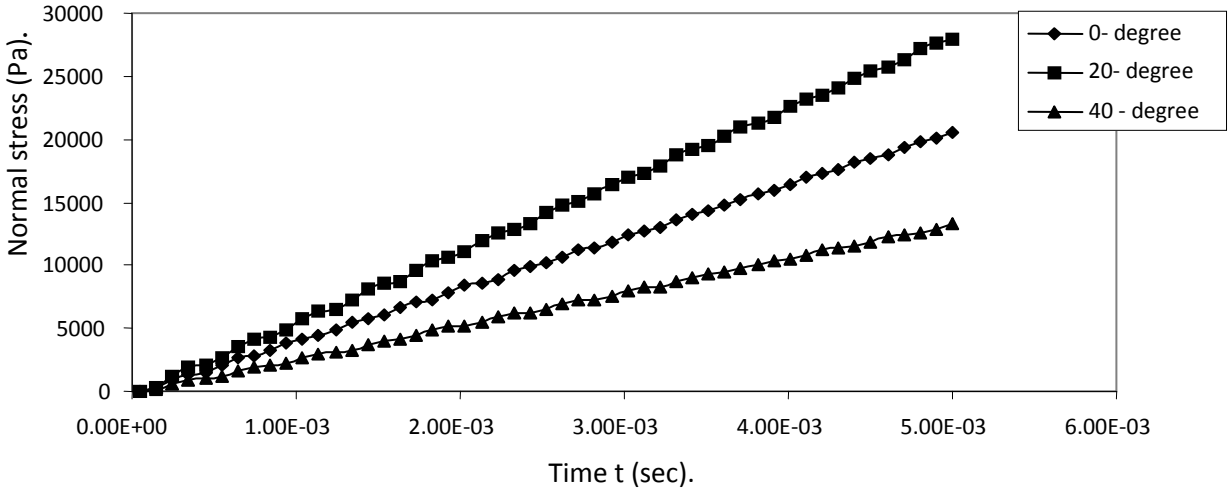

Figure(17):The effect of the lamination angle on the variation of normal stress at point (A) of square symmetric plate(4– Layers) with central circular hole under exponential-load.

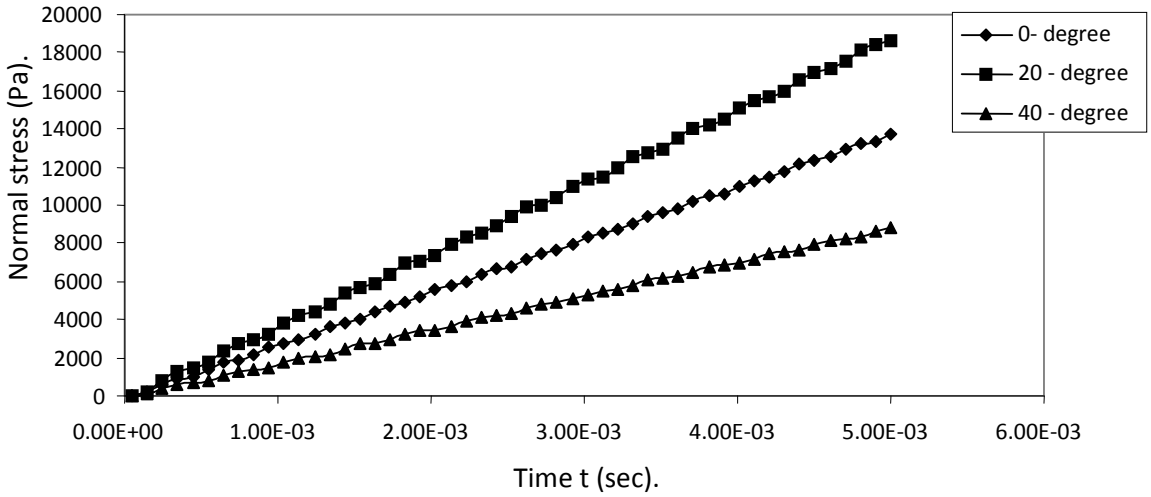

Figure(18):The effect of the lamination angle on the variation of normal stress at point (A) of square symmetric plate(6– Layers) with central circular hole under exponential-load.

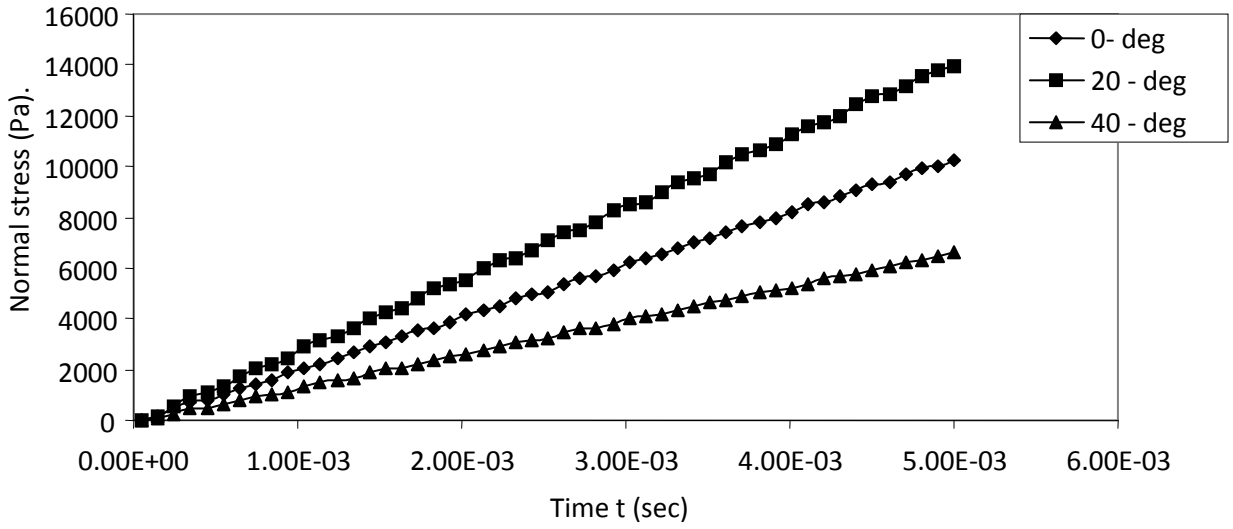

Figure(19): The effect of the Lamination angle on the variation of normal stress at point (A) of square plate (8 – Layers) with central circular hole under exponential-load

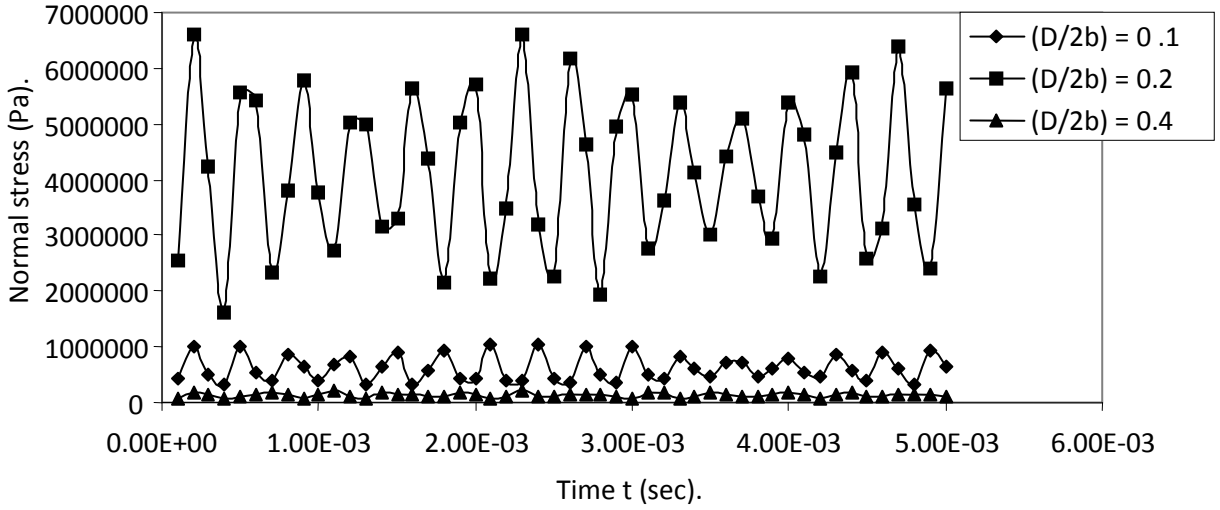

Figure(20): The effect of the (D/2b) ratio on the variation of normal stress at point (A) of square symmetric plate (4- layers) with central circular hole under step-load.

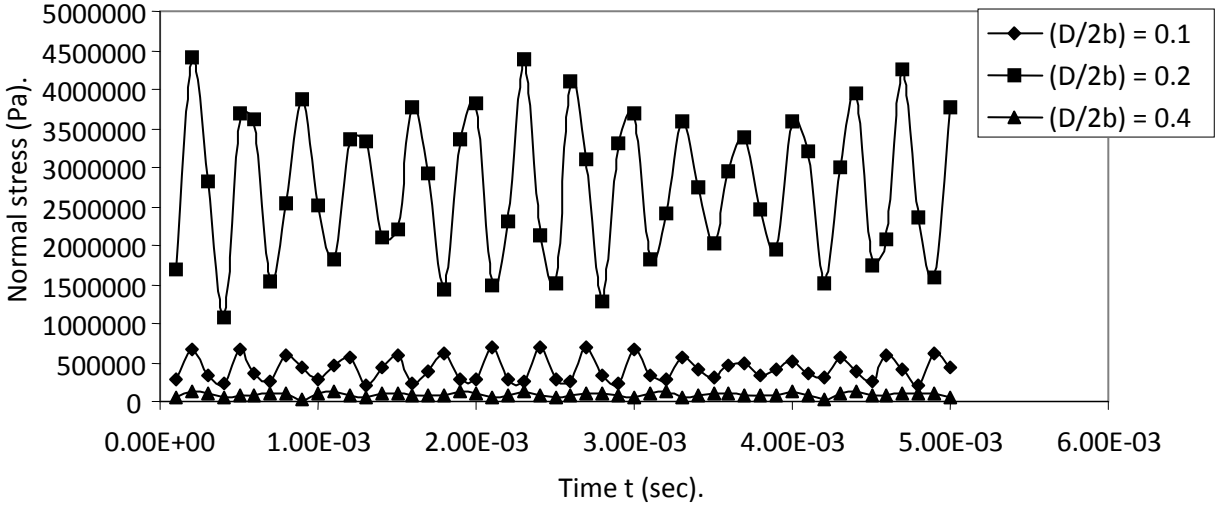

Figure(21): The effect of the (D/2b) ratio on the variation of normal stress at point (A) of square symmetric plate (6- layers) with central circular hole under step-load.

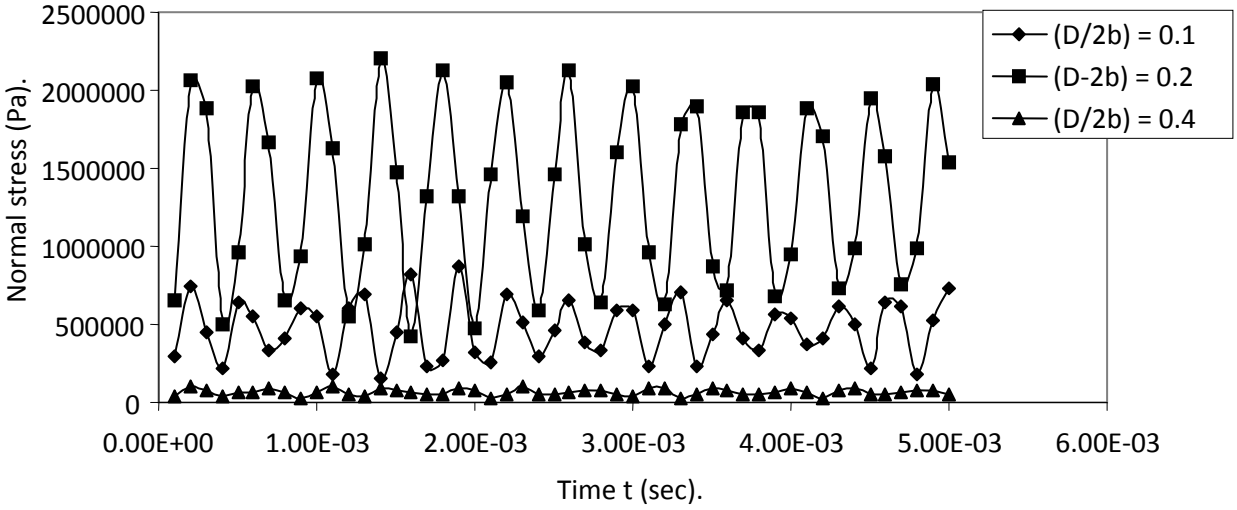

Figure(22): The effect of the (D/2b) ratio on the variation of normal stress at point (A) of square symmetric plate (8- layers) with central circular hole under step-load.

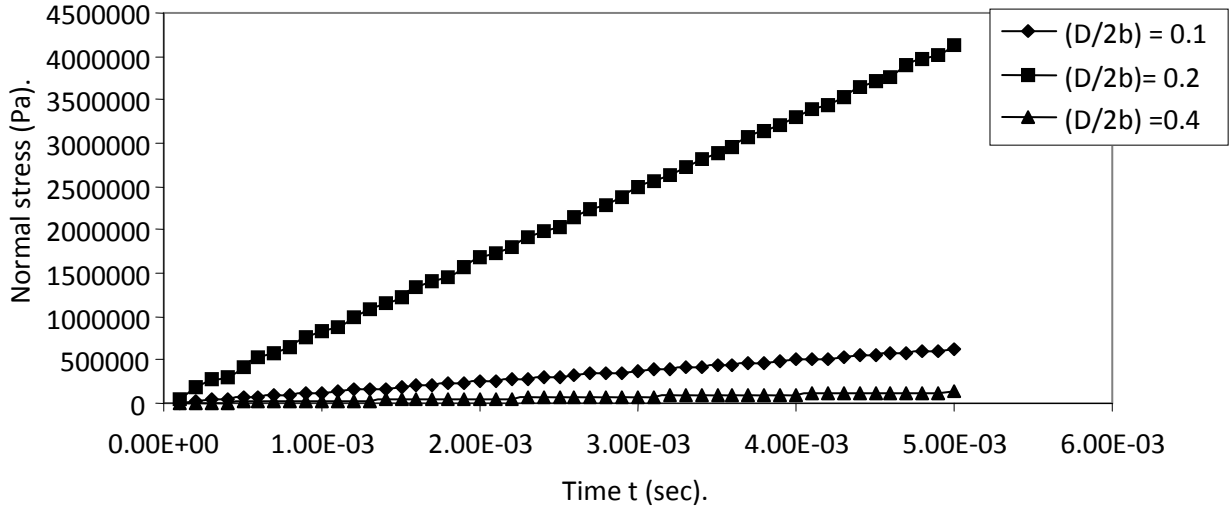

Figure(23): The effect of the (D/2b) ratio on the variation of normal stress at point (A) of square symmetric plate (4- layers) with central circular hole under ramp-load.

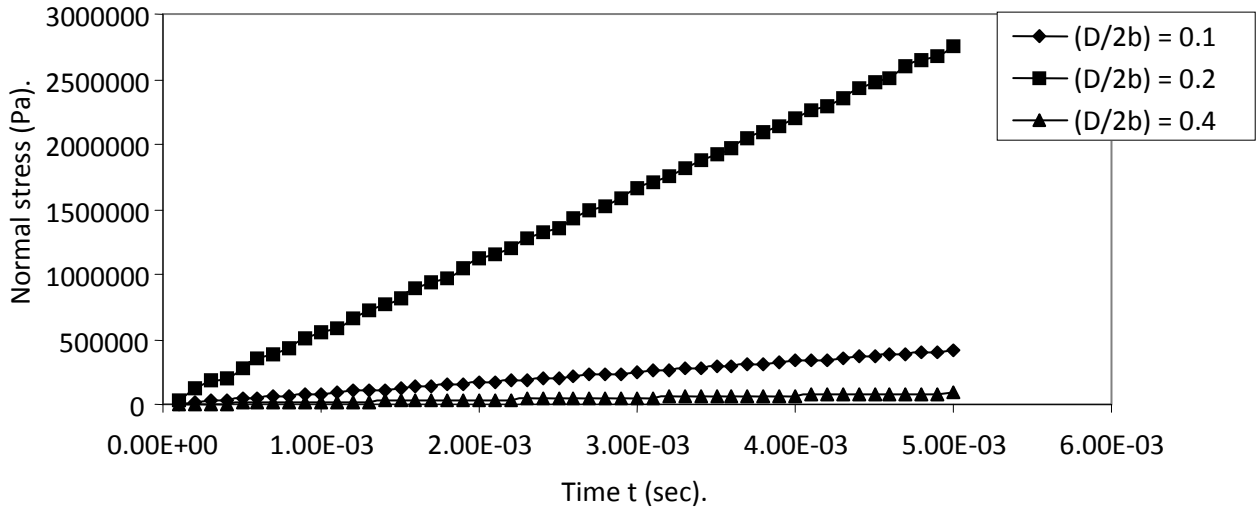

Figure(24):The effect of the (D/2b) ratio on the variation of normal stress at point (A) of square symmetric plate (6- layers) with central circular hole under ramp-load.

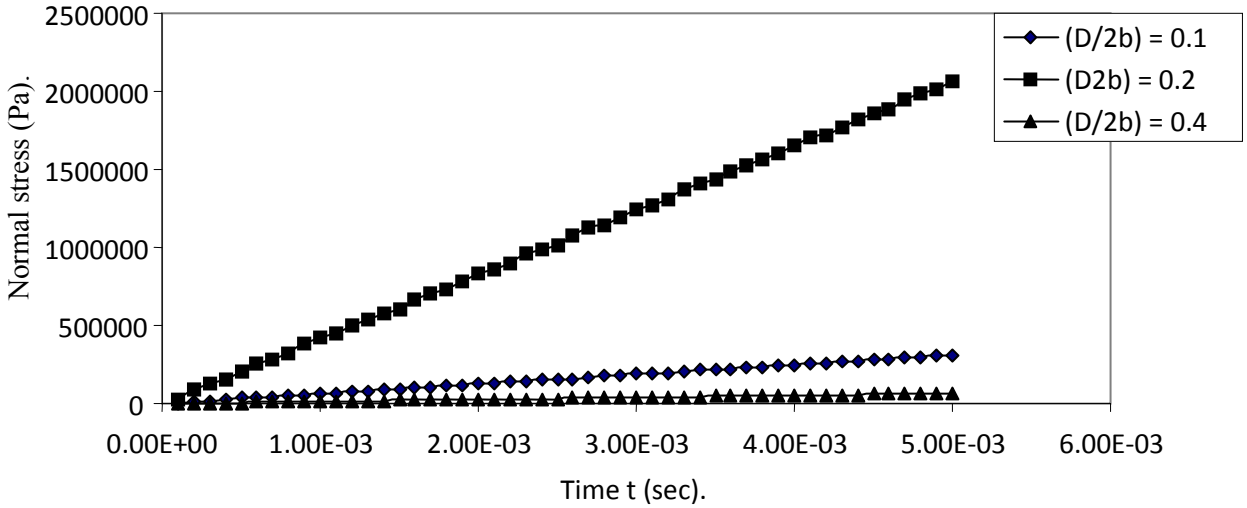

Figure(25): The effect of the (D/2b) ratio on the variation of normal stress at point (A) of square symmetric plate (8- layers) with central circular hole under ramp-load.

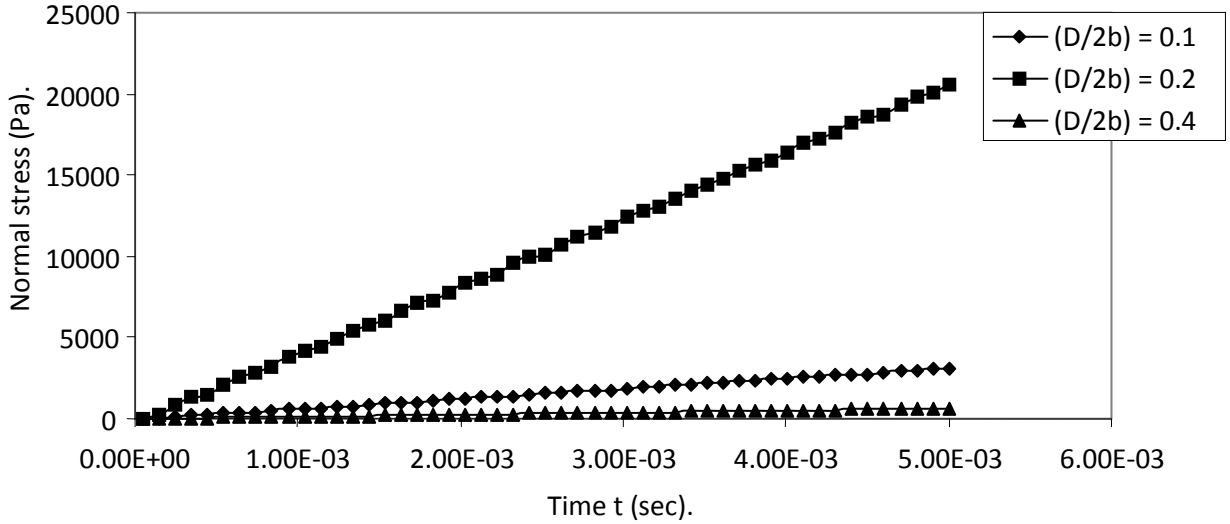

Figure(26):The effect of the (D/2b) ratio on the variation of normal stress at point (A) of square symmetric plate (4- layers) with central circular hole under exponential-load.

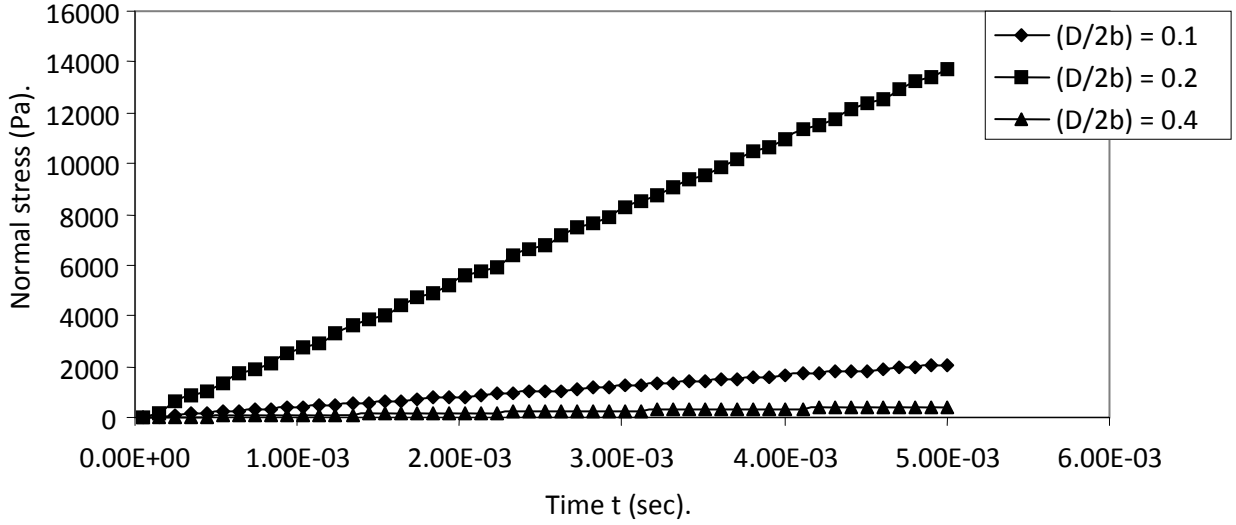

Figure(27): The effect of the (D/2b) ratio on the variation of normal stress at point (A) of square symmetric plate (6- layers) with central circular hole under exponential-load

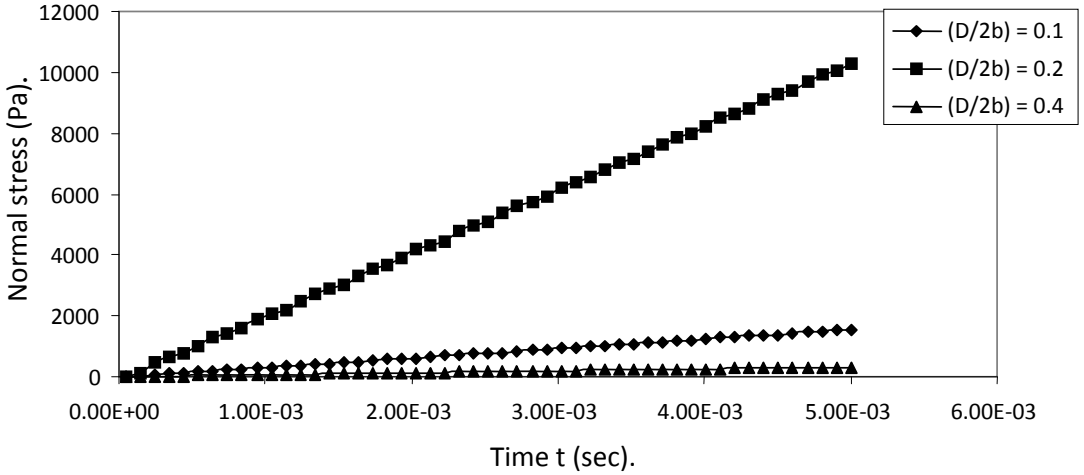

Figure(28): The effect of the (D/2b) ratio on the variation of normal stress at point (A) of square symmetric plate (8- layers) with central circular hole under exponential-load.

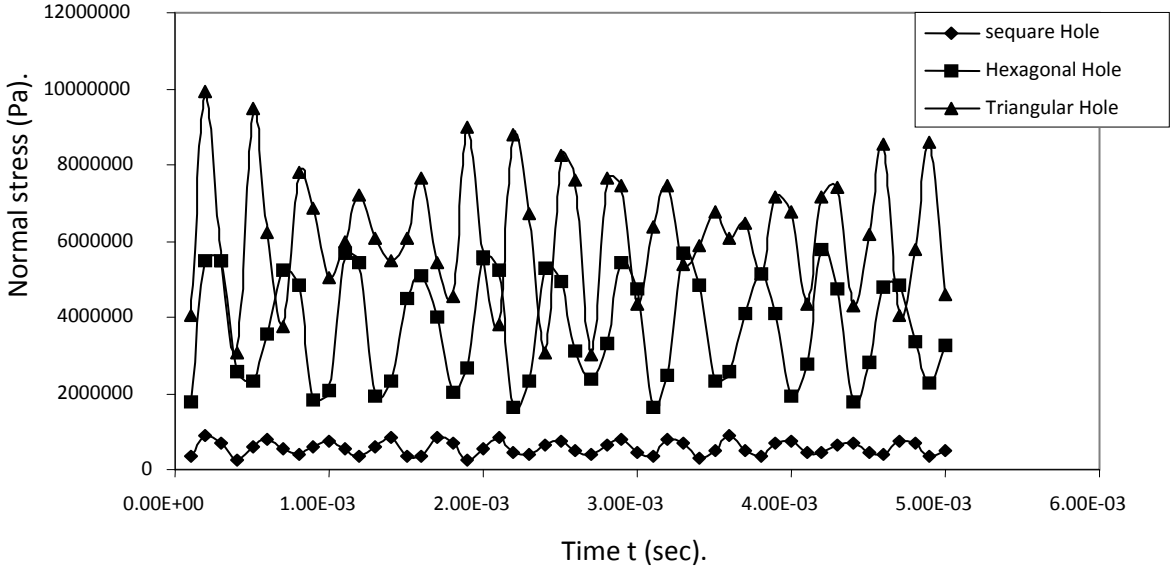

Figure(29): The effect of the shape of cut-out on the variation of normal stress at point (A) of square symmetric plate (4- layers) with different central hole under step-load.

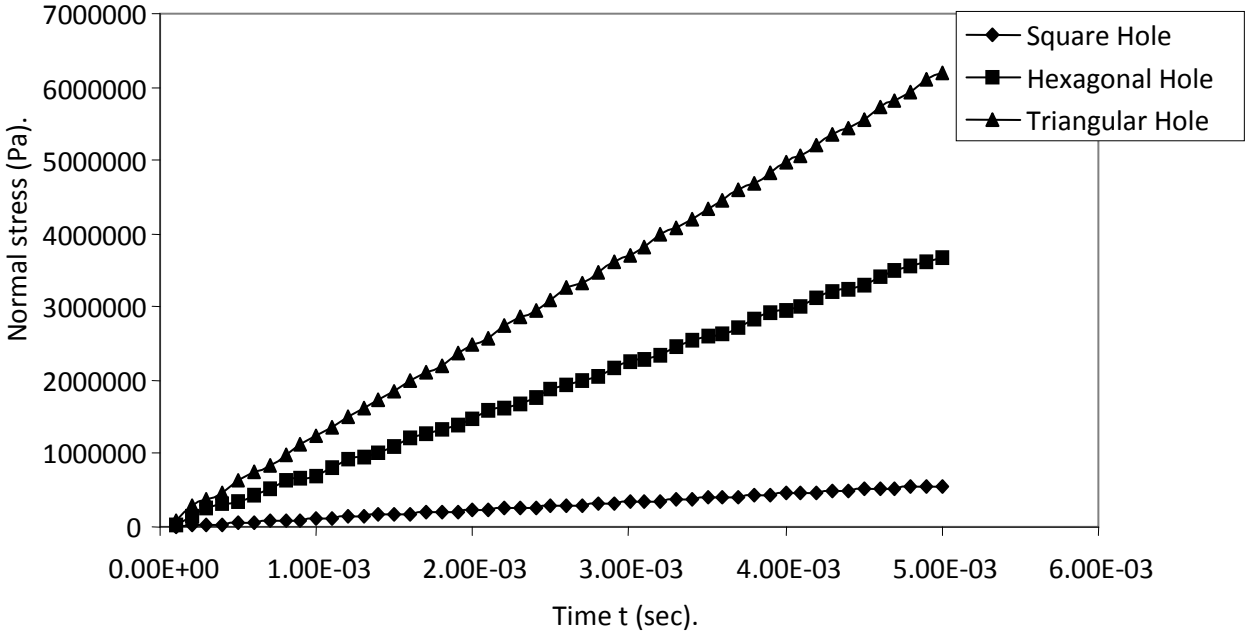

Figure(30):The effect of the shape of cut-out on the variation of normal stress at point (A) of square symmetric plate (4- layers) with different central hole under ramp-load.

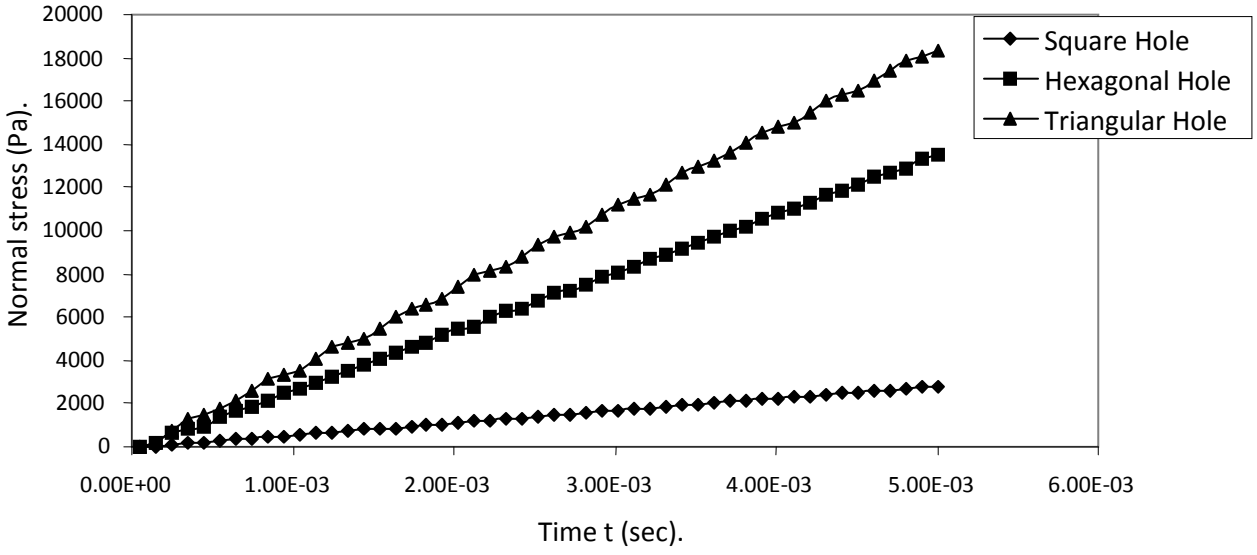

Figure(31): The effect of the shape of cut-out on the variation of normal stress at point (A) of square symmetric plate (4- layers) with different central hole under exponential

التحليل العابر للصفائح المركبة بمختلف أنواع القطوع

أ.د.محسن جبر جويج
قسم الهندسة الميكانيكية– كلية الهندسة
جامعة النهرين

أ.م.د.رياح نجم كطر
قسم الهندسة الميكانيكية – كلية الهندسة
جامعة الانبار

م.م أحمد نوري عويد

الخلاصــة.

تم تحليل الصفائح المركبة الناتجة من لصق عدد من الطبقات من المواد المسماة بمواد التقوية الليفية تحت تأثير الأحمال الديناميكية بمختلف القيم لعدد الطبقات وشكل وأبعاد الجزء المقطوع وزاوية التركيب ونوع التحميل. تم إنجاز العمل باستخدام البرنامج الهندسي المعروف ***(ANSYS)*** .

تم تقييم صلابة الصفائح المركبة على أساس قيمة الإجهاد عند الحافة الداخلية للجزء المقطوع وباتجاه التحميل. وجد أن هذه الصلابة تزداد بزيادة عدد الطبقات وعند قيمة (40^o) لزاوية التركيب واختيار قيمة ***(0.4)*** لأبعاد الجزء المقطوع وتفضيل الشكل المربع و/أو تجنب الشكل المثلث.

كذلك وجد أن الصفائح المركبة تصبح حساسة أكثر لمعدل الانفعال في حالة التحميل الخطي المتزايد (***ramp***) أو في حالة العدد القليل للطبقات أو عندما يكون شكل الجزء المقطوع مثلثاً.